NOLTR 69-31

A SPLITTER PLATE FOR THE PREVENTION OF VORTEX SHEDDING BEHIND FINITE CIRCULAR CYLINDERS IN UNIFORM CROSS FLOW

10 JULY 1967

NOL

UNITED STATES NAVAL ORDNANCE LABORATORY, WHITE OAK, MARYLAND

NOLTR 69-31

A SPLITTER PLATE FOR THE PREVENTION OF VORTEX SHEDDING BEHIND FINITE CIRCULAR CYLINDERS IN UNIFORM CROSS FLOW

Prepared by:
Dirse W. Sallet

ABSTRACT: Vortex shedding of circular cylinders in uniform cross flow may be prevented by the installation of a radially extending plate, which is rigidly attached to the cylinder. The principle of vortex shedding prevention by such a splitter plate is explained and the minimum dimensions of the plate are theoretically derived and compared with experimentally found values.

PUBLISHED 10 JULY 1967

U. S. NAVAL ORDNANCE LABORATORY
WHITE OAK, MARYLAND

NOLTR 69-31 10 July 1967

A SPLITTER PLATE FOR THE PREVENTION OF VORTEX SHEDDING BEHIND FINITE CIRCULAR CYLINDERS IN UNIFORM CROSS FLOW

This report presents a method of vortex shedding prevention from circular cylinders in uniform flow.

The task was part of a general investigation of the motions of a mine case and attempts to partially prevent such motions, when the weapon is in its moored position and currents exist.

All experimental work was performed in the Hydroballistics Tank of the U. S. Naval Ordnance Laboratory, White Oak.

E. F. SCHREITER
Captain, USN
Commander

A. E. Seigel
A. E. SEIGEL
By direction

CONTENTS

ILLUSTRATIONS

TABLES

LIST OF SYMBOLS

A	projected area of cylinder
C_D	coefficient of drag
D	diameter of cylinder
f	frequency of vortex shedding
F_D	drag force
h	lateral vortex spacing in a Kármán vortex street
ℓ	longitudinal vortex spacing in a Kármán vortex street
L	length of cylinder
L'	height of splitter plate
L_s-1	length of splitter plate in cylinder radii
P_n	stagnation point n (n = 1, 2, 3, 4 and 5)
R	Reynolds number
S	Strouhal number based on the diameter D and the velocity U
u	velocity component in x-direction
U	approach velocity
v	velocity component in y-direction
V	velocity of vortices relative to the fluid
w	complex potential
x_n	x-coordinate of vortex n
x_{max}	x-coordinate of y_{max} position
y_n	y-coordinate of vortex n
y_{max}	maximum distance of the zero stream line from the x-axis
z	complex function $z(x,y) = x + iy$ where $i = \sqrt{-1}$

$\bar{z}$	conjugate of z
Γ	circulation of vortex
κ	strength of vortex
ρ	density of fluid
ρ_c	average density of cylinder
ρ_R	$\rho_R = \frac{\rho + \rho_c}{\rho}$
φ	velocity potential
ψ	stream function

INTRODUCTION

When a bluff body is brought into the flow of a real fluid, vortex shedding will occur once a certain Reynolds number is exceeded. For a circular cylinder this Reynolds number is about 50. The frequency of shedding may be expressed as

$$f = S \frac{U}{D} \tag{1}$$

where the Strouhal number S is a function of the Reynolds number. Roshko (ref. 1) found

$$S = 0.212 \left(1 - \frac{21.2}{R}\right) \text{ for } 50 < R < 150 \tag{2}$$

and

$$S = 0.212 \left(1 - \frac{12.7}{R}\right) \text{ for } 300 < R < 2{,}000 \tag{3}$$

while for the range of Reynolds numbers from 2,000 to 400,000 the Strouhal number is reported to lie between 0.195 and 0.210 (ref. 2). A further increase in Reynolds numbers shows a transition zone,

$$4 \times 10^5 < R < 3.5 \times 10^6 \tag{4}$$

where the Strouhal number has been observed to lie between 0.21 and 0.46. For Reynolds numbers larger than 3.5×10^6 vortex shedding occurs with a Strouhal number of 0.27 (ref. 3).

The magnitude of the fluctuating force, the so-called Kármán force is

$$F_K = \tfrac{1}{2} C_K \rho A U^2 \tag{5}$$

where the coefficient C_K is usually assumed to be at least equal to 1.0 (ref. 4). Drescher (ref. 5) measured the unsteady pressure distribution of cylinders in cross flow, verifying the order of magnitude of the just stated assumption.

The detrimental effect the Kármán force may have on engineering structures became apparent by the collapse of a large suspension bridge, which was subjected to a moderate, steady wind. Other less dramatic and therefore less publicized failures are those of antennas, transmission lines and smoke stacks. The reoccurrence of such failures is usually prevented by the installation of appropriate damping devices. In certain engineering applications, however, a change of the vibrational system, e.g., additional damping, is not sufficient,

and the total neutralization of the Karman forces by fluid dynamical means may be desirable.

In the following it will be shown that vortex shedding may be prevented and therefore the fluctuating Karman forces may not occur, by the installation of a splitter plate. The minimum dimensions of such a fin for a finite cylinder will be derived and compared with the experimentally determined optimum dimensions. It should be realized, however, that a self-excited vibration may occur, e.g., on bodies with lift surfaces or with active mechanical systems, even though there is no periodic vortex shedding on the body which is initially steady. Preventing vortex shedding will eliminate the "switching mechanism" (ref. 6) most often responsible for the occurrence of the self-excited vibration of a body (other than airfoil shaped) in steady fluid flow.

STABILITY ANALYSIS

The underlying principle of the method by which a splitter plate of sufficient length and infinitesimal thickness will tend to inhibit vortex shedding becomes plausible from a stability analysis carried out by L. Foppl (ref. 7) in 1913.

Let the complex potential for two-dimensional flow be

$$w(z) = \varphi(x,y) + i\psi(x,y) \tag{6}$$

Then the complex velocity is

$$\frac{dw}{dz} = u - iv \tag{7}$$

where

$$u = \frac{\partial \varphi}{\partial x} = \frac{\partial \psi}{\partial y} \tag{8}$$

and

$$v = \frac{\partial \varphi}{\partial y} = -\frac{\partial \psi}{\partial x} \tag{9}$$

A closed circular stream line, with a radius equal to unity, representing the cylinder in uniform flow is formed by the complex potential

$$w_c = U\left(z + \frac{1}{z}\right) \tag{10}$$

while the potential of vortex 1 and vortex 2 is

$$w_1 = +iK \log\left(z - z_1\right) \tag{11}$$

$$w_2 = - iK \log \left(z - z_2\right) \tag{12}$$

To retain the unit circle as a stream line (see fig. 1) when adding equations (10), (11) and (12), the images of vortices 1 and 2 (with respect to the circle)

$$w_{11} = - iK \log \left(z - z_{11}\right) \tag{13}$$

and

$$w_{22} = + iK \log \left(z - z_{22}\right) \tag{14}$$

must be included (Thomson's theorem). Summing equations (10) through (14) yields

$$w = U\left(z + \frac{1}{z}\right) + iK \log \frac{(z - z_1)(z - z_{22})}{(z - z_2)(z - z_{11})} \tag{15}$$

It should be pointed out, that by choosing a cylinder with a unit radius, all distances are expressed in radii.

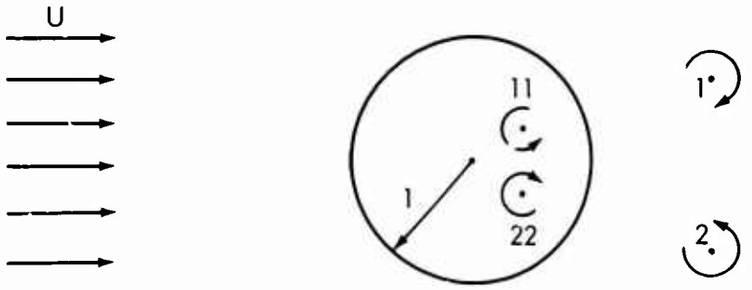

Fig. 1 Nomenclature of Vortices

According to Thomson's principle

$$z_{11} = \frac{1}{\bar{z}_1} \tag{16}$$

and

$$z_{22} = \frac{1}{\bar{z}_2} \tag{17}$$

so that

$$x_{11,22} = \frac{x_{1,2}}{x_{1,2}^2 + y_{1,2}^2} \tag{18}$$

and

$$y_{11,22} = \frac{y_{1,2}}{x_{1,2}^2 + y_{1,2}^2} \tag{19}$$

By setting the propagation velocities of the vortices 1 and 2 equal to zero, Föppl (ref. 7) obtained

$$\pm 2y_{1,2} = r_{1,2} - \frac{1}{r_{1,2}} \tag{20}$$

and

$$\kappa = 2 \cdot U y_{1,2} \left(1 - \frac{1}{r_{1,2}^4}\right) \tag{21}$$

where

$$r_{1,2} = \sqrt{x_{1,2}^2 + y_{1,2}^2} \tag{22}$$

and

$$r_1 = r_2 \tag{23}$$

since x_1 equals x_2 and y_1 equals $-y_2$ for the here assumed symmetrical case.

Equation (20) gives the loci at which the two vortices must be, if they are stationary with respect to the cylinder (see fig. 2). Equation (21) correlates the strength κ of such a stationary vortex with its position behind the circular cylinder and the free-stream velocity U. It is seen, that for a constant free-stream velocity the vortex strength increases as the vortex pair moves away from the cylinder on the Föppl vortex path. Rubach's flow visualization experiments (ref. 8) agree with the theory developed by Föppl.

In order to determine whether equation (20) represents a stable equilibrium position of the vortices, vortices 1 and 2 are displaced by a small distance from their position on the Föppl path; a return to their original location means that this position is one of stable equilibrium. For a small symmetrical disturbance of the vortices (the x - axis being the axis of symmetry) Föppl (ref. 7) obtained

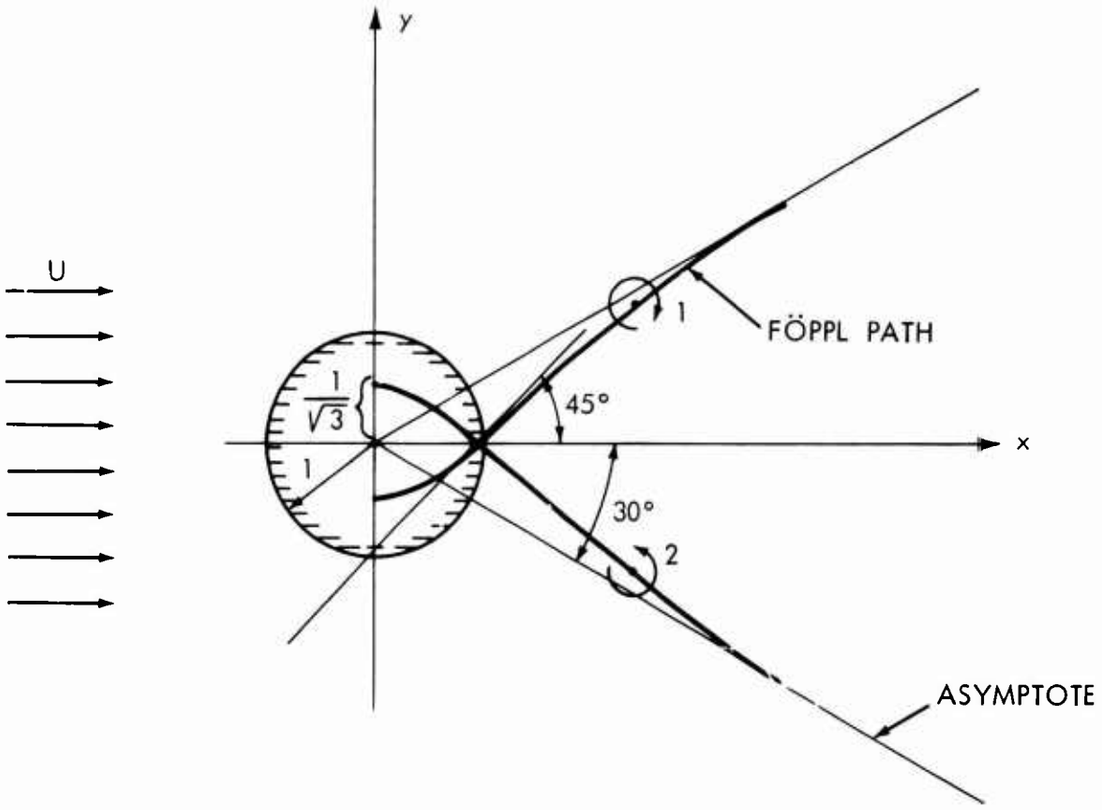

Fig. 2 Location of Vortices

$$\frac{d^2\alpha}{dt^2} + (Y - A)\frac{d\alpha}{dt} + (BX - AY)\,\alpha = 0 \qquad (24)$$

after replacing u by $\frac{d\alpha}{dt}$, v by $\frac{d\beta}{dt}$, x by $x + \alpha$ and y by $y + \beta$ in the equations representing the propagation velocities of the vortices. Here

$$A = -\frac{2U}{r^6}\,x\,(4y^2 + 1) \qquad (25)$$

$$B = \frac{2U}{r^5}\left(r^4 + 2r^2 + \frac{2y^2}{r^2}\right) \qquad (26)$$

$$X = 8x^2y\,\frac{U}{r^6(r^4 - 1)} \qquad (27)$$

and

$$Y = \frac{2xU}{r^4}\left(1 + \frac{4y^2}{r^2(r^4 - 1)}\right) \tag{28}$$

The indices on x, y and r have been omitted. The general solution of equation (24) is

$$\alpha = C_1 \cdot \exp\left(\lambda_1 t\right) + C_2 \exp\left(\lambda_2 t\right) \tag{29}$$

where

$$\lambda_{1,2} = -\frac{Y - A}{2} \pm \tfrac{1}{2}\sqrt{(Y - A)^2 - 4\,(BX - AY)} \tag{30}$$

Stability is therefore proven, since

$$\left.\begin{array}{r} Y > A \\ \text{and} \\ (BX - AY) > 0 \end{array}\right\} \tag{31}$$

A similar stability investigation, for the case for which the symmetry of the vortices with respect to the x - axis is not preserved, yields instability of the displaced vortices.

The above considerations show that a pair of vortices may be at rest behind a circular cylinder in uniform flow. If this is the case, they will position themselves according to equations (20) and (21), where the latter equation relates position with vortex strength and free-stream velocity. When a small disturbance acts upon these vortices, the vortices will swing back to their original position on the Föppl path, if the disturbance is of such a manner that it results in a displacement of the vortices which is symmetrical with respect to the x - axis. A disturbance producing an unsymmetrical displacement with respect to the x - axis results in instability of the vortices. The typically staggered Kármán vortex street is usually formed in this case.

The reason why a splitter plate may prevent vortex shedding is now apparent: Due to the image effect of the plate all vortex displacements will be symmetrical with respect to the x - axis (see fig. 3).

SPLITTER PLATE DIMENSIONS

The question now arises what the optimum dimensions of such a splitter plate should be, in order to prevent vortex shedding. The answer to this question is important to the practical application of this method of vortex shedding prevention.

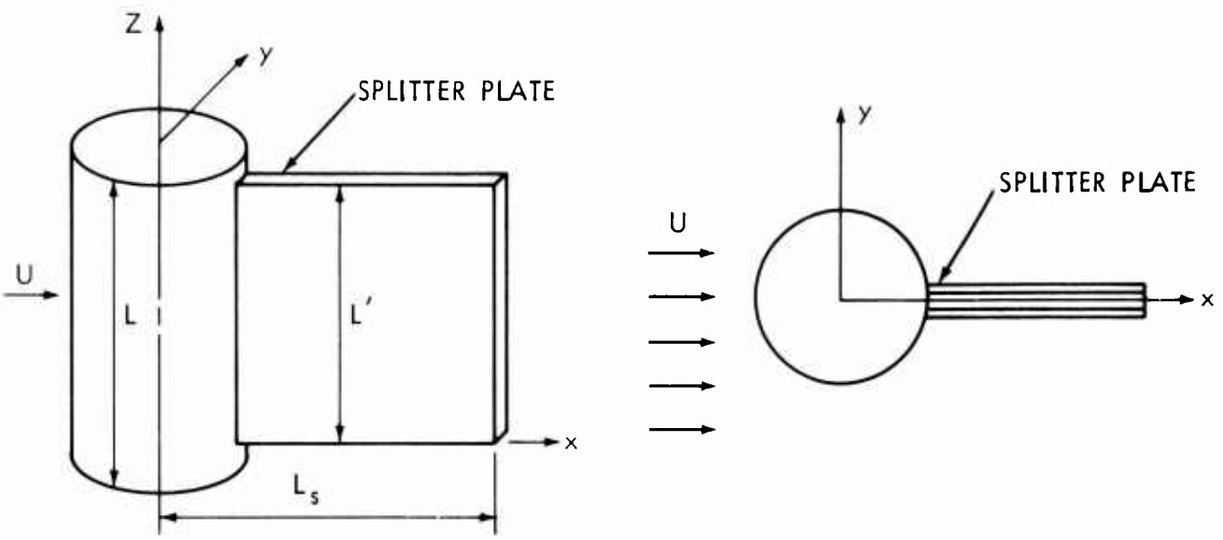

Fig. 3 Splitter Plate

The optimum dimensions are the shortest length and the shortest height of the splitter plate which will prevent vortex shedding in the real fluid in which the cylinder moves with uniform velocity. A simple experimental trial and error type investigation would eventually yield the optimum dimensions of the particular cylinder tested. It is desirable, however, to deduce from theoretical considerations the minimum plate dimensions defined below. Such considerations will not only shorten the experimental investigation but will also yield valuable results of general character.

The minimum fin length (L_s-1) which will insure the separation of the fluid moving with the vortices is given by the location of the rear stagnation point P_3 (see fig. 4). This minimum fin length which is defined for the non-viscous two dimensional flow field is shorter than the optimum fin length which was defined for the real, viscous flow in consideration. The difference between the minimum fin length and the optimum fin length is not only caused by viscous effects; a finite displacement of vortex 1 or 2 in the downstream direction will require a corresponding increase in the minimum fin length to insure complete separation of the two fluid bodies moving with the circular zero stream line representing the cylinder. An expression for the distance L_s may now be derived (see also ref. 8). Separating equation (15) into real and imaginary parts and comparing with equation (6) yields:

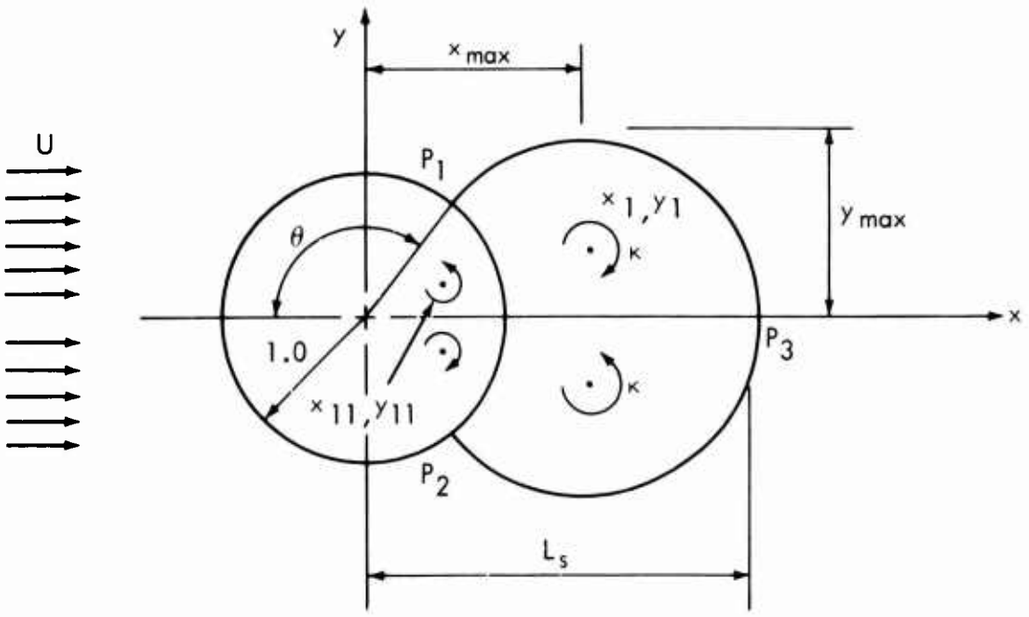

Fig. 4 Location of Stagnation Points P_n

$$\Phi = U\left(x + \frac{x}{x^2 + y^2}\right) + \kappa \left(\arctan \frac{y + y_1}{x - x_1} + \arctan \frac{y - y_{11}}{x - x_{11}} - \arctan \frac{y - y_1}{x - x_1} - \arctan \frac{y + y_{11}}{x - x_{11}}\right) \tag{32}$$

and

$$\Psi = U\left(y - \frac{y}{x^2+y^2}\right) + \kappa \log \sqrt{\frac{\left[(x-x_1)^2+(y-y_1)^2\right]\left[(x-x_{11})^2+(y+y_{11})^2\right]}{\left[(x-x_1)^2+(y+y_1)^2\right]\left[(x-x_{11})^2+(y-y_{11})^2\right]}} \tag{33}$$

By performing the operations indicated in equations (8) and (9) the velocities in the x - and y - directions are found to be:

$$u = U\left(1 - \frac{x^2-y^2}{(x^2+y^2)^2}\right) + \kappa\left[\frac{y - y_1}{(x-x_1)^2+(y-y_1)^2} + \frac{y + y_{11}}{(x-x_{11})^2+(y+y_{11})^2} - \frac{y + y_1}{(x-x_1)^2+(y+y_1)^2} - \frac{y - y_{11}}{(x-x_{11})^2+(y-y_{11})^2}\right] \tag{34}$$

$$-v = \frac{2U\,x\,y}{\left(x^2+y^2\right)^2} + K\left[\frac{x-x_1}{\left(x-x_1\right)^2+\left(y-y_1\right)^2} + \frac{x-x_{11}}{\left(x-x_{11}\right)^2+\left(y+y_{11}\right)^2} - \frac{x-x_1}{\left(x-x_1\right)^2+\left(y+y_1\right)^2} - \frac{x-x_{11}}{\left(x-x_{11}\right)^2+\left(y-y_{11}\right)^2}\right] \tag{35}$$

Equating equation (34) to zero and setting

$$y = 0$$

and

$$x = L_s$$

gives the required expression containing the term L_s,

$$1 - \frac{1}{L_s^2} + \frac{2K}{U}\left[\frac{y_{11}}{\left(L_s - x_{11}\right)^2 + y_{11}^2} - \frac{y_1}{\left(L_s - x_1\right)^2 - y_1^2}\right] = 0 \tag{36}$$

To determine the value of L_s from (36) the location of the vortices and the ratio $\frac{K}{U}$ must be known. However, since a stationary vortex pair exists, only one vortex coordinate must be given or be assumed, as equation (20) determines the second coordinate and equation (21) then in turn determines the corresponding $\frac{K}{U}$ ratio. Conversely, if the ratio of vortex strength to free-stream velocity is known, the position of stationary vortices may then be calculated with equations (20) and (21), and equation (36) may again be solved for L_s.

From the above discussion it is apparent that, if the numerical value for L_s is to be obtained, either the vortex position or the ratio of vortex strength to free-stream velocity must be assumed. In this article the following assumptions are considered:

1. The $\frac{K}{U}$ ratio of a stationary vortex is the same as that of a single vortex in a Kármán vortex street. This assumption will give a smaller than actual $\frac{K}{U}$ ratio, which is apparent from a simple energy consideration; therefore, a smaller than adequate length L_s will result.

2. The stagnation points P_1 and P_2 coincide with the positions of boundary-layer separation of a circular cylinder in uniform flow (see fig. 4). In this case the splitter plate length will vary

substantially, depending on whether a laminar or a turbulent boundary layer, giving early or delayed separation respectively, exists.

3. The distance $2y_{max}$ (see fig. 4) is the same as the width of the wake behind a long circular cylinder of equivalent diameter.

4. The vortices behind the cylinder have the same lateral spacing as the vortices in a staggered Kármán vortex street.

For the first of the above-stated assumptions, a value of $\frac{\kappa}{U}$ for a single vortex of a Kármán vortex street must be deduced. The strength of a line vortex is

$$\kappa = \frac{\Gamma}{2\pi} \tag{37}$$

where

$$\Gamma = 2V\ell \cdot \operatorname{cotan} \frac{\pi h}{\ell} \tag{38}$$

Substituting the Kármán stability value

$$\frac{h}{\ell} = 0.281 \tag{39}$$

(ref. 9) into equation (38) gives

$$\Gamma = 2 \cdot \sqrt{2}\ell V \tag{40}$$

Applying the Kronauer stability criterion, the velocity V may be expressed in terms of the velocity U. For the vortex spacing ratio given in equation (39), a ratio of

$$\frac{V}{U} = 0.14 \tag{41}$$

is obtained (ref. 10), which is the same value observed by von Kármán in his original experiments supporting his theory (ref. 9). The vortex strength to free-stream velocity may now be expressed as

$$\frac{\kappa}{U} = \frac{0.14\sqrt{2}}{\pi}\ell \tag{42}$$

The longitudinal vortex spacing ℓ in a Kármán vortex street is shown to be (Appendix A)

$$\ell = 0.86 \frac{D}{S} \tag{43}$$

or

$$\ell = \frac{D}{2S}\left[1 + \sqrt{1 - \frac{C_D\, S^2}{0.397}}\right] \qquad (44)$$

depending on whether equation (41) is assumed to be correct or if one relies only upon empirically found values for the drag coefficient and the Strouhal number. The results obtained by equations (43) and (44) are in close agreement with each other and with the experimental evidence (Appendix A). For the Reynolds number range $2 \times 10^4 < R < 2 \times 10^5$ the generally accepted values for a long circular cylinder are $S = 0.195$ and $C_D = 1.20$, resulting in the numerical value for ℓ of 4.31D. Since the radius of the cylinder was defined to be unity, ℓ equals 8.62 and the required ratio is

$$\frac{K}{U} = 0.542 \qquad (45)$$

Table 1 shows the resulting length L_s, the position of the vortices and stagnation points, the $\frac{K}{U}$ ratio and the coordinates of the maximum width of the zero stream line.

The second assumption to be investigated is based on the geometrical similarity of the potential and real fluid flow fields. Terminating the Blasius power series with the fifth term, separation $\left(\frac{du}{dy} = 0\right)$ occurs at $\theta = 110^\circ$, when potential flow velocity is assumed to exist (ref. 11). Actually measured values of the separation points not only depend upon the flow regime but also upon the definition of the point of separation. Fage (ref. 12) shows that the visually observed separation of the boundary layer may take place as much as 10° downstream from the angle θ determined by the point on the cylinder at which inflection of the velocity profile occurs $\left(\frac{du}{dy} = 0\right)$. In real fluids separation takes place further upstream in the laminar flow regime and further downstream in the turbulent flow regime, due to the particular pressure distribution formed. For this and the above reasons a variety of values for θ have been assumed and the corresponding flow field characteristics computed as shown in Table 1. Since geometrical similarity is emphasized the visually observed separation point should be used when calculating the minimum fin length in this case.

The third assumption compares the wake width of the real fluid with the maximum width of the zero stream line of the potential flow field. For the specific parameters the reader is again referred to Table 1. Based on Roshko's result (ref. 13) that the wake Strouhal number for circular cylinders is 0.16, the wake width in a Reynolds number range of 2×10^4 to 2×10^5 is 1.2 diameters. Above the critical Reynolds number the wake is found to be 0.5 diameter wide.

The fourth assumption proposes the same lateral vortex spacing of the real, staggered Kármán vortex street and the two vortices behind

TABLE 1
FLOW FIELD PARAMETERS*

ϕ	x_1	y_1	x_{11}	y_{11}	$\frac{\kappa}{U}$	L_s	x_{max}	y_{max}	Assumption
95.0	11.514	6.597	0.0654	0.0375	13.194	22.94	11.513	13.756	
100.0	5.836	3.270	0.1304	0.0731	6.537	11.5	5.835	6.825	
105.0	3.968	2.144	0.1951	0.1054	4.278	7.68	3.965	4.474	
110.0	3.058	1.575	0.2584	0.1331	3.127	5.78	3.052	3.283	2 (laminar boundary layer - potential flow velocity)
115.0	2.520	1.221	0.3214	0.1558	2.403	4.62	2.510	2.544	
115.2	2.503	1.21	0.3239	0.1566	2.380	4.58	2.492	2.520	4 (laminar boundary layer)
120.0	2.169	0.980	0.3829	0.1730	1.899	3.85	2.153	2.036	
125.0	1.920	0.800	0.4438	0.1848	1.514	3.28	1.897	1.660	
129.5	1.750	0.67	0.4984	0.1908	1.231	2.88	1.719	1.389	4 (turbulent boundary layer)
130.0	1.738	0.661	0.5025	0.1911	1.212	2.85	1.708	1.370	2 (turbulent boundary layer)
133.7	1.634	0.578	0.5440	0.1924	1.028	2.60	1.597	1.20	3 (laminar boundary layer)
135.0	1.598	0.549	0.5596	0.1923	0.964	2.50	1.560	1.136	
140.0	1.482	0.452	0.6171	0.1883	0.748	2.22	1.436	0.937	
145.0	1.382	0.365	0.6761	0.1787	0.5560	1.97	1.329	0.756	
145.7	1.375	0.359	0.6807	0.1776	0.5421	1.95	1.321	0.743	1 (Kármán vortex)
150.0	1.3067	0.297	0.7277	0.1653	0.4096	1.77	1.250	0.658	
155.3	1.2370	0.232	0.7809	0.1465	0.2791	1.59	1.15	0.50	3 (turbulent boundary layer)
160.0	1.186	0.183	0.8236	0.1273	0.1898	1.46	0.952	0.360	

* All length dimensions are expressed in cylinder radii, and all angles are given in degrees.

the cylinder. Using the mean values for ℓ as obtained from equations (43) and (44) by substituting the coefficients

$$S = 0.195 \qquad C_D = 1.20 \qquad \text{for} \qquad 2 \times 10^4 < R < 2 \times 10^5$$

and

$$S = 0.370 \qquad C_D = 0.35 \qquad \text{for} \qquad R \approx 10^6$$

the y - coordinates for the vortex positions on the Föppl path become $y_1 = 1.21$ and $y_1 = 0.67$ for the above-indicated cases, respectively.

The second dimension of the splitter plate L' may be estimated by relating the decrease in the coefficient of drag of a finite cylinder to the decrease in vortex length parallel to the axis of the cylinder (Appendix A):

$$L' = \frac{C_D \text{ (finite L/D)}}{C_D \text{ (infinite L/D)}} L \qquad (46)$$

DISCUSSION

Inspection of Table 1 shows that assumptions 2 and 4 result in similar flow fields not only when a laminar but also when a turbulent boundary layer exists. Assumptions 1 and 3 also result in flow fields having parameters of approximately the same magnitude; here it is noticed that the values obtained by assumption 1 lie between those obtained by assumption 3 which vary according to the type of existing boundary layer.

Experiments performed with water as a medium support the theoretical results as obtained with assumptions 2 and 4. A cylinder with an L/D ratio of 5.15 and a density ratio ρ_R equal to 1.85 was towed at different speeds in a large tank and its motions filmed (see fig. 5). For towing speeds for which the Reynolds number based on the cylinder diameter was below the critical, a splitter plate of length 3D corresponding to L_s equal to 7 was sufficient to eliminate all motions induced by the vortex shedding, while test runs with a fin of length 2D (equivalent to $L_s = 5$) showed the typical oscillating motions of a bare cylinder. While the 3D fin stayed aligned with the direction of flow (all fins were rigidly attached to the cylinder), the 2D fin supported an oscillation of the cylinder around its longitudinal axis. For velocities for which the Reynolds numbers were well above the critical, a splitter plate of 1.5D ($L_s = 4.0$) was sufficient to suppress all vortex induced motions. The above theoretical considerations tend to give a less than necessary splitter plate length rather than the exact or even a longer than necessary length. The reason for this was already discussed. The experiments were performed in the new NOL Hydroballistics Tank (ref. 22).

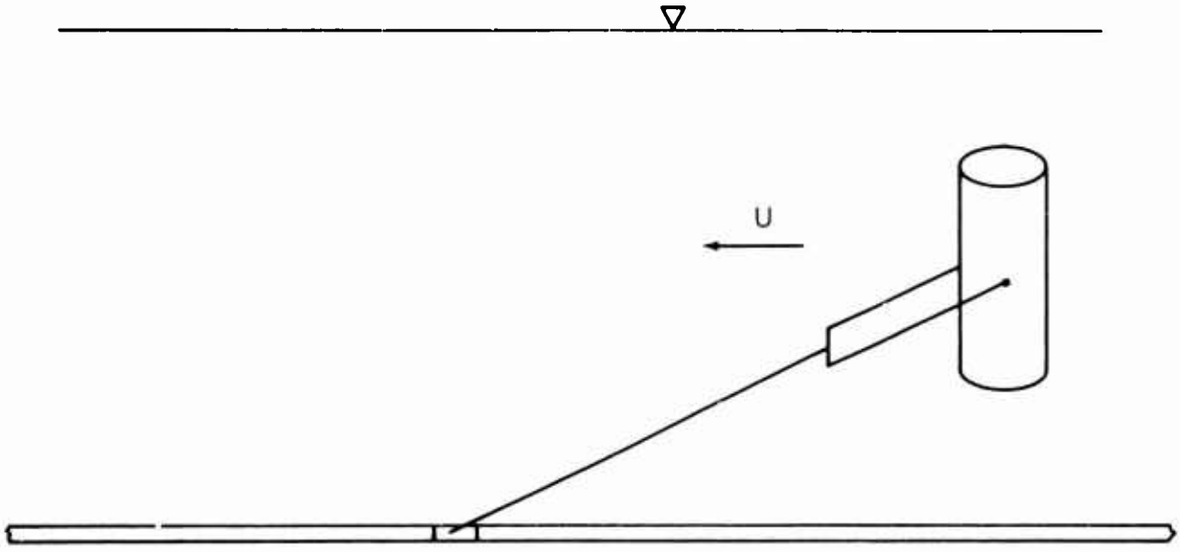

Fig. 5 Test Arrangement

It should be pointed out that the observation of the motion of the cylinder is not a direct observation of the vortex shedding and its prevention by a splitter plate, but rather an observation of the reaction of a complex, self-excitable vibrational system when vortex shedding has been inhibited to various degrees by different splitter plates. Experimental evidence based on flow visualization should therefore be obtained. Towing tests were also performed using different cable lengths, changing the natural frequency of the pendulum-like system (see fig. 5). In this manner it was assured that the natural frequency and the vortex shedding frequency (possibly reduced to a finite value due to the splitter plate according to reference 14) were of such magnitudes that the typical self-excited vibration with large amplitudes would have occurred. Meier-Windhorst (ref. 15) shows that the frequency range for which the large amplitudes occur is strongly dependent upon the density ratio ρ_R, becoming wider as ρ_R approaches 2. The same important trend was noticed by Glass (ref. 16), again supporting the validity of a deduction of the flow field in view of vortex shedding from the observations of the motion of the cylinder.

The above-described tests also indicated that the other minimum dimension of the splitter plate is $L' \approx 0.9L$ for subcritical flow and $L' = L$ for velocities where the Reynolds number exceeds the critical, as was expected from equation (46) in conjunction with the drag data of circular cylinders having the indicated slenderness ratio (e.g., ref. 17).

APPENDIX A

KÁRMÁN VORTICES BEHIND BLUFF BODIES

The longitudinal spacing of Kármán vortices due to a submerged bluff body in uniform flow may be deduced by combining generally accepted empirical data with the results of von Kármán's vortex street and drag theories. The following plausible assumptions are made:

Assumption A-1: The submerged body is of uniform cross section and has a large enough slenderness ratio so that a two-dimensional flow analysis is justified.

Assumption A-2: A regular Kármán vortex street is generated by the uniform motion of the submerged bluff body.

Assumption A-3: The drag force experienced by the submerged body is only due to the generated vortex street and not due to the viscous forces acting directly on the body.

Let the velocity of the object in motion be U and the velocity of the shed vortices be V (see fig. A-1). The shedding frequency

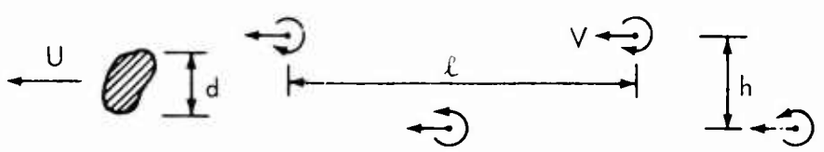

Fig. A-1 Kármán Vortex Street

f is:

$$f = \frac{U-V}{\ell} \qquad \text{(A-1)}$$

From direct experimental observation:

$$f = \frac{U}{D} S \qquad \text{(A-2)}$$

The Strouhal number S as a function of the Reynolds number has been determined for plates and circular cylinders by various investigators (ref. 18, 1, 2, 19 and 3). Equating the frequencies given by equations (A-1) and (A-2) yields:

$$\frac{1 - \frac{V}{U}}{\ell} = \frac{S}{D} \qquad \text{(A-3)}$$

If the velocity of the vortex street V is known, equation (A-3) may directly be solved for the required longitudinal vortex spacing ℓ in terms of the free-stream velocity U and the characteristic width D of the body. The vortex velocity V can only be measured by flow visualization, by hot-wire methods or by similar techniques. Such measurements, which are usually quite cumbersome to perform, may then, of course, yield directly the vortex spacing. However, the ratio $\frac{V}{U}$ can be expressed as a function of ℓ, D, and the coefficient of drag C_D as follows: von Kármán (ref. 9) showed, by equating the drag force acting on the body to the change of momentum of the generated infinite vortex street, that

$$F_D = \left[\rho\Gamma(U - 2V)\frac{h}{\ell} + \rho\frac{\Gamma^2}{2\pi\ell}\right] L \qquad (A\text{-}4)$$

With the assumptions A-2 and A-3 equation (A-4) may be rewritten in the following form (ref. 17):

$$C_D = 2\left[0.794\frac{V}{U} - 0.314\left(\frac{V}{U}\right)^2\right]\frac{\ell}{D} \qquad (A\text{-}5)$$

Since

$$\frac{V}{U} \ll 1 \qquad (A\text{-}6)$$

see, for example, reference 18, $\left[0.314\left(\frac{V}{U}\right)^2\right]$ is negligible when compared to $\left[0.794\frac{V}{U}\right]$. Equation (A-5) becomes:

$$\frac{V}{U} = \frac{C_D D}{1.588\,\ell} \qquad (A\text{-}7)$$

Substituting the above velocity ratio into equation (A-3) yields

$$\ell = \frac{D}{2S}\left(1 + \sqrt{1 - \frac{C_D S}{0.397}}\right) \qquad (A\text{-}8)$$

The alternative minus sign in front of the radical in equation (A-8) was eliminated, since for flows below the critical Reynolds number all observed vortex streets due to bluff bodies are wider than the width of the body, and for flows above the critical Reynolds number, the lateral vortex street dimension approaches that of the width of the body.

A simple method of deducing ℓ as a function of S and D only, suggests itself from the work of Bearman (ref. 10). By writing the Kronauer stability criterion in the form

$$\left(\frac{\partial C_D}{\partial \frac{h}{\ell}}\right)_{\frac{V}{U} = \text{const.}} = 0 \qquad \text{(A-9)}$$

Bearman derived the following relationship between $\frac{h}{\ell}$ and $\frac{V}{U}$.

$$2 \cosh \frac{\pi h}{\ell} = \left(\frac{V}{U} - 2\right) \sinh \frac{\pi h}{\ell} \left(\cosh \frac{\pi h}{\ell} \sinh \frac{\pi h}{\ell} - \frac{\pi h}{\ell}\right) \qquad \text{(A-10)}$$

For the von Kármán stability condition, ($\frac{h}{\ell} = 0.281$) the velocity ratio $\frac{V}{U}$ becomes 0.14. This is the identical value observed by von Kármán (ref. 9) in the experiments to support his theory. Substituting this value into equation (A-3) yields

$$\ell = 0.86 \frac{D}{S} \qquad \text{(A-11)}$$

Therefore, by assuming Kronauer's stability criterion to hold true, one of the variables of equation (A-8) is eliminated.

Table A-1 shows the vortex spacing behind circular cylinders. Directly measured values for the longitudinal vortex spacing are given by Fage and Johanson (ref. 18); for the Reynolds number range 2×10^4 to 2×10^5 a value of ℓ equal to 4.27 D was observed. In this range equation (A-8) approximates the vortex spacing better than equation (A-11). The two unknown parameters in equation (A-3) are the Strouhal number S and the velocity ratio $\frac{V}{U}$. While equation (A-11) relies only upon one experimentally determined parameter to express ℓ as a function of D, namely, the Strouhal number S, equation (A-8) relies on two experimentally determined parameters, namely, the coefficient of drag C_D and the Strouhal number S. It is interesting to note that the value of the dimensionless product of $C_D S$ is nearly constant over a wide Reynolds number range (see Table A-1).

When a finite bluff body is brought into uniform flow, so-called "down-wash" will occur at the ends of this body due to the low back pressure. Clearly, the flow is now three dimensional and assumption A-1 is therefore disregarded. In view of assumptions A-2 and A-3 and neglecting additional three dimensional effects, the length L in equation (A-4) must now be replaced by the modified length L'. The ratio of the modified length L' (the length of the vortices) and the actual length of the body L is obtained from the drag data:

$$L' = \frac{C_D(\text{finite L/D})}{C_D(\text{infinite L/D})} L \qquad \text{(A-12)}$$

For the case of a circular cylinder, the coefficients of drag for the infinite (1:∞) and finite (1:5) cylinders are as follows (ref. 17):

Table A-1: Longitudinal Vortex Spacing Behind Circular Cylinders

R	S	C_D	S C_D	ℓ after Eq (A-8)	ℓ after Eq (A-11)
100	0.168 (ref. 1)	1.40 (ref. 2)	0.235	4.88 D	5.12 D
1,000	0.211 (ref. 1)	1.00 (ref. 11)	0.211	3.99 D	4.08 D
2,000	0.215 (ref. 19)	0.95 (ref. 2)	0.204	3.95 D	4.00 D
10,000	0.205 (ref. 19)	1.11 (ref. 2)	0.228	4.03 D	4.20 D
$2x10^4$-$2x10^5$	0.195 (ref. 2)	1.20 (ref. 11)	0.234	4.21 D	4.41 D
10^6	0.370 (ref. 3)	0.35 (ref. 3)	0.130	2.46 D	2.32 D

$$\left.\begin{aligned} C_D(1{:}\infty) &= 1.2 \\ C_D(1{:}5) &= 0.75 \end{aligned}\right\} \quad \text{for } 2 \times 10^4 < R < 2 \times 10^5$$

The modified length L' for this Reynolds number range and the given diameter to length ratio becomes L' = 0.625 L. For the circular cylinder of the given slenderness ratio, the values shown in reference 17 indicate that for $4 \times 10^2 < R < 2 \times 10^5$ a minimum modified length L' (min.) occurs at $R = 4 \times 10^3$ and is equal to 0.88L; for Reynolds numbers above the critical number, L' seems to equal L.

Most experiments investigating the spacing ratio of the Kármán vortex street show a much larger value for $\frac{h}{l}$ than that predicted by von Kármán. In other words, experimental evidence seems to question assumption A-2. Hooker (ref. 20) discusses the action of viscosity in increasing the spacing ratio; while the centers of vorticity appear to remain closely in the von Kármán arrangement, the centers of rotation of the eddies (which are observed) move outwards. Hooker also points out that the longitudinal spacing remains surprisingly constant, so that the observed increase in the apparent spacing ratio is due to the increasing lateral distance between the centers of rotation of the created eddies.

Assumption A-3 is supported by the work of Schiller and Linke (ref. 21). This investigation shows that at a Reynolds number of 5,000 the viscous effects on cylinders account for 5 percent of the total drag, while at a Reynolds number of 40,000 this value has decreased to 2 percent.

Of interest is the investigation by von Kármán in which he shows that by fixing all vortices except one vortex pair, this free vortex pair will assume the considerably larger spacing ratio of $\frac{h}{l} = 0.36$. This seems to explain the observed shorter longitudinal spacing l for the first 3 or 4 vortices immediately after the vortex shedding body. The correcting factor by which l must be multiplied (see equation (A-8) or (A-12)) to give the longitudinal vortex spacing immediately behind the body is 0.78.

APPENDIX B

REFERENCES

1. Roshko, A., "On the Development of Turbulent Wakes From Vortex Streets", NACA Report 1191, 1952

2. Goldstein, S., (editor), Modern Developments in Fluid Dynamics, Oxford University Press, Oxford, 1938

3. Roshko, A., "Experiments on the Flow Past a Circular Cylinder at Very High Reynolds Number", J. Fluid Mech. 10, 1961, p. 345-356

4. Den Hartog, J. P., "Recent Technical Manifestations of von Kármán's Vortex Wake", Proc. N.A.S., Vol. 40, 1954

5. Drescher, H., "Messung der auf quergeströmte Zylinder ausgeübten zeitlich veränderten Drücke", Z. f. Flugwissenschaften, Vol. 4, 1956, p. 17-21

6. Magnus, K., Schwingungen, B. G. Teubner Verlagsgesellschaft mbH, Stuttgart 1961

7. Föppl, L., "Wirbelbewegung hinter einem Kreiszylinder", Sitzungsb. d. bayr. Akad., 1913, p. 1-17

8. Rubach, H. L., "Ueber die Entstehung und Fortbewegung des Wirbelpaares hinter zylindrischen Korpern", Forschungsarbeiten auf dem Gebiete des Ingenieurwesens, VDI, Heft 185, 1916

9. Kármán, Th. von, and Rubach, H., "Über den Mechanismus des Flüssigkeits- and Luftwiderstandes", Physik. Zeitschrift Vol. 13, 1912, p. 49-59

10. Bearman, P. W., "On Vortex Street Wakes", NPL AERO Report 1199, 1966

11. Schlichting, H., "Boundary Layer Theory", Verlag G. Braun, Karlsruhe, 1955

12. Fage, A., "The Airflow Around a Circular Cylinder in the Region Where the Boundary Layer Separates from the Surface", Aeronaut. Research Comm., R. and M. 1179, 1928

13. Roshko, A., "On the Drag and Shedding Frequency of Two-Dimensional Bluff Bodies", NACA TN 3169, 1954

14. Roshko, A., "On the Wake and Drag of Bluff Bodies", J. Aero. Sciences, Vol. 22, 1955, p. 124-132

15. Meier-Wirdhorst, A., "Flatterschwingungen von Zylindern im gleichmässigen Flüssigkeitsstrom", Mitteilungen des Hydraulischen Instituts der Technischen Hochschule München, Heft 9, 1939

16. Glass, R., "A Study of the Self-Excited Vibrations of Spring Supported Cylinders in a Steady Fluid Stream", Doctoral Thesis, University of Maryland, 1966

17. Wien-Harms, Handbuch der Experimentalpysik, (Vol. 4 part 2) Akademische Verlagsgesellschaft M.B.H., Leipzig, 1931

18. Fage, A., and Johanson, F. C., "The Structure of Vortex Streets", Phil. Mag. S. 7, Vol. 5, No. 28, 1928, p. 417-441

19. Kovasznay, L. S. G., "Hot-Wire Investigation of the Wake Behind Cylinders at Low Reynolds Numbers", Proc. Roy. Soc Ser. A, Vol. 198, 1949, p. 174-190

20. Hooker, S. G., "On the Action of Viscosity in Increasing the Spacing Ratio of a Vortex Street", Proc. Roy, Soc. Ser. A, Vol. 154, 1935, p. 67-89

21. Schiller, L., and Linke, W., "Druck- und Reibungswiderstand des Zylinders bei Reynoldsschen Zahlen 5000 bis 40,000," Z. f. Flugtechnik und Motorluftschiffahrt, Nr. 7, Vol. 24, 1933, p. 193-198

22. Seigel, A. E., "The Hydroballistics Facility at NOL," NOLTR 66-125 (1966)

UNCLASSIFIED

Security Classification

DOCUMENT CONTROL DATA - R & D

(Security classification of title, body of abstract and indexing annotation must be entered when the overall report is classified)

1. ORIGINATING ACTIVITY (Corporate author)

U. S. Naval Ordnance Laboratory

2a. REPORT SECURITY CLASSIFICATION

UNCLASSIFIED

2b. GROUP

--

3. REPORT TITLE

A SPLITTER PLATE FOR THE PREVENTION OF VORTEX SHEDDING BEHIND FINITE CIRCULAR CYLINDERS IN UNIFORM CROSS FLOW

4. DESCRIPTIVE NOTES (Type of report and inclusive dates)

5. AUTHOR(S) (First name, middle initial, last name)

Dirse W. Sallet

6. REPORT DATE	7a. TOTAL NO. OF PAGES	7b. NO. OF REFS
10 July 1967	26	21

8a. CONTRACT OR GRANT NO

b. PROJECT NO

c.

d.

9a. ORIGINATOR'S REPORT NUMBER(S)

NOLTR 69-31

9b. OTHER REPORT NO(S) (Any other numbers that may be assigned this report)

10. DISTRIBUTION STATEMENT

Distribution of this document is unlimited.

11. SUPPLEMENTARY NOTES

12. SPONSORING MILITARY ACTIVITY

13. ABSTRACT

Vortex shedding of circular cylinders in uniform cross flow may be prevented by the installation of a radially extending plate, which is rigidly attached to the cylinder. The principle of vortex shedding prevention by such a splitter plate is explained and the minimum dimensions of the plate are theoretically derived and compared with experimentally found values.

DD FORM 1 NOV 65 1473 (PAGE 1)

S/N 0101-807-6801

UNCLASSIFIED

Security Classification

14 KEY WORDS	LINK A		LINK B		LINK C	
	ROLE	WT	ROLE	WT	ROLE	WT
Vortex shedding						
Vortex prevention						
Splitter plate						
Karman vortices						
Cylinder flutter						
Moored mine						
Finite cylinder						
Induced vibrations						
Submerged cylinder						
Mine stability						